

Relaxation Pathways in Metallic Glasses

ISABELLA GALLINO^{1,2} and RALF BUSCH¹

1.—Chair of Metallic Materials, Department of Materials Science and Engineering, Saarland University, Campus C6.3, 66123 Saarbrücken, Germany. 2.—e-mail: i.gallino@mx.uni-saarland.de

At temperatures below the glass transition temperature, physical properties of metallic glasses, such as density, viscosity, electrical resistivity or enthalpy, slowly evolve with time. This is the process of physical aging that occurs among all types of glasses and leads to structural changes at the microscopic level. Even though the relaxation pathways are ruled by thermodynamics as the glass attempts to re-attain thermodynamic equilibrium, they are steered by sluggish kinetics at the microscopic level. Understanding the structural and dynamic pathways of the relaxing glassy state is still one of the grand challenges in materials physics. We review some of the recent experimental advances made in understanding the nature of the relaxation phenomenon in metallic glasses and its implications to the macroscopic and microscopic properties changes of the relaxing glass.

INTRODUCTION

From a thermodynamic point of view, metallic glasses are non-equilibrium systems, trapped during solidification via vitrification far from the thermal equilibrium before they can crystallize. In the solidification pathways schematically pictured in Fig. 1, the transition to the glassy state of the metastable liquid (path 2) can occur if crystallization (path 1) is bypassed. In contrast to the crystallization process, which is an equilibrium phase transformation and is characterized by a discontinuous change in the extensive properties, the glass transition is a continuous transformation in terms of volume, enthalpy and entropy changes. The glass transition is therefore a non-equilibrium transition that is usually understood as a structural arrest as the result of increasingly sluggish liquid kinetics upon supercooling. The higher the number of constituents and the larger the atomic mismatch, the more densely packed the structure of the supercooled liquid is and the more difficult the rearrangement of the atoms toward equilibrium becomes.¹ For these systems, the intrinsic or structural (α)-relaxation time, τ , grows dramatically during supercooling until a structural arrest occurs, as τ eventually surpasses the experimental observation time. On these time scales the liquid behaves like a solid, i.e., it does not exhibit viscous flow and a glass is formed. The drastic increase of τ with

supercooling in metallic glass-forming systems is manifested macroscopically by a non-Arrhenius equilibrium viscosity increase of several orders of magnitude, which is connected to a drastic increase of the apparent activation energy for viscous flow. The non-Arrhenius temperature dependence of the viscosity in the vicinity of the glass transition temperature, T_g , can be modeled by fitting the empirical Vogel–Fulcher–Tammann (VFT) equation, $\eta(T) = \eta_0 \exp[D^* T_0 / (T - T_0)]$, to the liquid viscosity equilibrium data. Here D^* is a measure of an inherent property of the liquid state as it approaches T_g , the so-called kinetic fragility.^{2,3} The VFT-equation reflects the degree of departure of the liquid dynamics from the Arrhenius equation, with smaller values of D^* corresponding to more kinetically fragile liquids. Bulk metallic glasses (BMGs) in general show fragile kinetics with D^* values between 13 and 26.^{4,5}

Depending on the applied cooling rate, the thermodynamic system of the glass occupies distinct local minima of an energy landscape that correspond to metastable low-temperature states. As a consequence, the thermodynamic fate of the glass is to spontaneously evolve with time toward the closest free energy minimum, i.e., the metastable supercooled liquid state on a long-time scale. Extensive thermodynamic and other physical properties, such as density, enthalpy or viscosity and electrical resistivity, slowly evolve with time as the glass

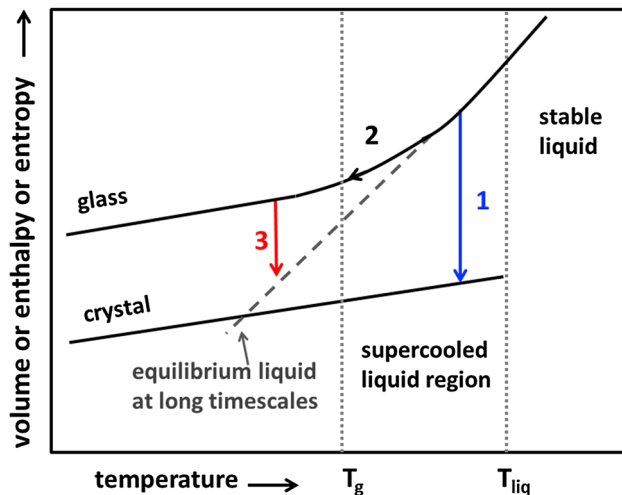


Fig. 1. Schematic diagram showing the change in volume or enthalpy during (1) crystallization, (2) vitrification and (3) physical aging below T_g .

attempts to re-attain thermodynamic equilibrium. The equilibrium is observed on long timescales, and the equilibrated glass behaves like a liquid. This is the process of physical aging and is ubiquitous among all types of glasses. The schematics of Fig. 1 show that the physical aging (path 3) has the effect of reducing the volume and the enthalpy of the glass toward a denser and more stable state. This densification upon relaxation in metallic glasses is connected to an increase of viscosity as the excess volume is annealed out (see, e.g., Refs. 6–12).

Distinct from physical aging is the process of *chemical aging*, which deals with the interaction of the surface with the environment over time or the development of chemical inhomogeneities, such as clustering or phase separation in the bulk. The study of both types of aging of glasses below T_g is not only of scientific interest, but also of great practical importance. For BMGs in particular, both physical and chemical aging can cause severe embrittlement¹³ and oxidation-induced crystallization,¹⁴ respectively. Both aging processes can enhance the fracture and fatigue of the final products.¹³ The ability to understand and characterize the mechanisms of aging in BMG systems is expected to play a central role in ensuring their success as commercial materials. This is also especially true in the application of metallic glasses in net-shape and additive methods such as selective imprinting and laser melting to produce amorphous metallic high-strength components with complex geometries. For these applications, elastic materials are needed, and BMGs are ideal candidates because they sustain larger elastic deformations than crystalline alloys because of low elastic modulus values and high elastic strength limits ($\sim 2\%$).

This article focuses on physical aging and addresses and reviews the macroscopic and microscopic methods used to characterize the change of extensive and intrinsic properties during physical aging. It discusses selected experimental results that recently have contributed to a better understanding of the nature and consequences of physical aging in metallic glasses, taking into consideration enthalpic, kinetic and structural aspects.

MACROSCOPIC RELAXATION PATHWAYS

As mentioned above, extensive and macroscopic physical properties, such as density, enthalpy and viscosity or electrical resistivity, slowly evolve with time during physical aging. Relaxation pathways of metallic glasses are usually studied using thermo-mechanical methods that can measure changes in length and viscosity or using differential scanning calorimetry to measure enthalpy changes. The change of physical properties during aging in metallic glasses is mostly observed to be non-exponential in nature.^{8–12,15–18} The response functions $\varphi(t)$ to an applied temperature are connected to spontaneous fluctuations of the equilibration process and exhibit highly stretched exponential behavior. For temperatures in the vicinity of T_g , the empirical Kohlrausch–William–Watts (KWW) equation, i.e., $\varphi(t) = \exp[-(t/\tau_{KWW})^{\beta_{KWW}}]$, is used to characterize the observed decay,^{19,20} where t is the annealing time, β_{KWW} ($0 < \beta_{KWW} < 1$) is the stretching exponent, and τ_{KWW} is the average relaxation time that describes the non-exponential equilibration kinetics. This relaxation time is the time for relaxation into equilibrium and should not be confused with the aforementioned intrinsic relaxation time τ . The KWW approach neglects non-linearity effects such as the structure dependence of the relaxation time.^{21–23} The origin of the non-exponential nature of the relaxation pathway is still highly debated, and several scenarios are taken into consideration. For example, one is that the stretched dynamic response is understood as the result of spatially heterogeneous regions that each relax exponentially with a characteristic distinct relaxation time.^{24,25}

Viscosity and Volume Relaxation

The time dependence of the isothermal viscosity of BMG in the vicinity of T_g is detected using the isothermal three-point beam-bending method in a thermal mechanical analyzer (TMA). This is a well-established and reliable method to obtain equilibrium viscosity data, which are essential to experimentally determine the kinetic fragility of the glass-forming system. An example is shown in Fig. 2a for the $Mg_{65}Cu_{23}Y_{10}$ BMG.⁸ The method was applied successfully in numerous studies of BMGs by Busch and co-workers.^{5–11} In earlier studies it was shown that the final relaxed state is equivalent to the

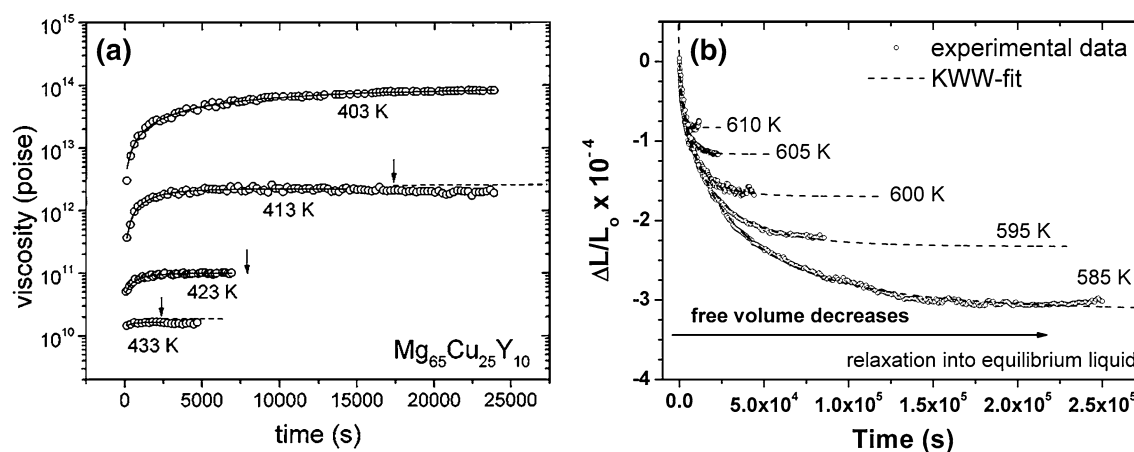


Fig. 2. Isothermal thermomechanical measurements in the glass transition region. (a) Viscosity change detected using the three-point beam-bending method for the $\text{Mg}_{65}\text{Cu}_{25}\text{Y}_{10}$ BMG composition.⁸ (b) Experimental relative changes in length of the $\text{Zr}_{44}\text{Ti}_{11}\text{Ni}_{10}\text{Cu}_{10}\text{Be}_{25}$ BMG composition.¹⁰ The dashed curves are the fits to the KWW equation.

supercooled state if observed on a long timescale and that the relaxation pathway can be understood as an isothermal glass transition.^{7,8,26}

The volumetric contraction of glassy specimens during the isothermal structural relaxation can be measured by dilatometry in a TMA. This method is used to obtain information regarding the excess volume (free volume) frozen in the glass during the vitrification pathway and to obtain a value for the total reduction of the excess volume during relaxation below T_g . The structural relaxation is assumed to occur isotropically, and thus the relative change in the volume of the glassy specimen during annealing can be directly obtained by studying the relative change in length, $\Delta L(t)/L_0$. As an example, Fig. 2b shows the time evolution of the length relaxation of a Zr-based BMG as it physically ages.¹⁰ The data are fit with the KWW equation (dashed lines). Evenson and Busch have shown that there is a remarkable agreement between the way the excess volume relaxes as obtained from volumetric relaxation measurements and the relaxation kinetics calculated from viscosity measurements. Furthermore, both quantities are directly connected to the enthalpy change during relaxation.¹⁰

Enthalpy Relaxation

Thermodynamically, the glassy state drifts toward a state of lower free energy during annealing and the system lowers its enthalpy. The kinetics of enthalpy release during relaxation can be directly studied by analyzing the calorimetric signal recorded during isothermal calorimetric measurements below T_g . The isothermal baseline of the crystallized sample is subtracted from the isothermal heat flow signal of the relaxing sample and integrated as a function of time to obtain the enthalpy relaxation functions, $\Delta H(t)$, as described in the details in Ref. 16. Figure 3 shows the enthalpy relaxation curves obtained for the Zr-based BMG

Vit106a by fitting the $\Delta H(t)$ functions with the KWW equation. The total exothermic enthalpy change increases with decreasing annealing temperature, and at the same time a longer time for relaxation and a smaller value of β are observed. The stretching exponent β increases monotonously with increasing temperature and approaches unity close to the calorimetric glass transition as plotted in the inset, indicating that at T_g all relaxation modes are converging into one single exponential decay.

It is important to note that prior to enthalpy relaxation experiments, the influence of the thermal history on the glass transition temperature should be minimized by applying a standard treatment to the sample, as demonstrated in Ref. 27. To assure the same enthalpic state for each specimen, the as-cast material must be heated to above the end of the calorimetric glass transition and cooled with a controlled standard rate, q_c . After completion of annealing, the sample is first cooled down and then re-heated with a rate $q_h = q_c$ to the end of the crystallization process for the detection of the enthalpy recovery, which is described in details in the following paragraph.

Enthalpy Recovery

We have shown that the same amount of enthalpy that is released during relaxation is recovered back into the system when the relaxed glass is heated up through the glass transition.¹⁶ The enthalpy recovery signal manifests itself as an endothermic overshooting of the heat flow signal that is associated to the glass transition process. An example of how the endothermic overshooting signal is evolving with annealing time is given in the inset plot of Fig. 4. Precise enthalpy recovery values are obtained from the integration of the overshooting signal of aged glasses with respect to the heat flow signal of an unrelaxed or standard treated material. The enthalpy recovery method requires a high thermal

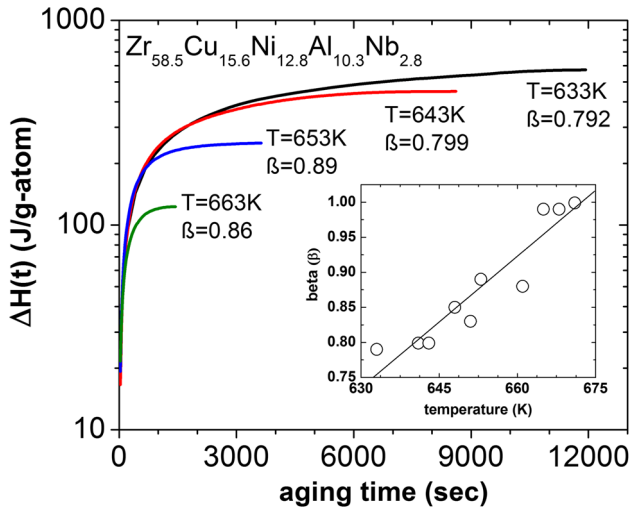


Fig. 3. Isothermal enthalpy relaxation curves for the $Zr_{58.5}Cu_{15.6}Ni_{12.8}Al_{10.3}Nb_{2.8}$ BMG composition.¹⁶ The $\Delta H(t)$ functions are modeled with the KWW equation resulting in a β exponent that reaches unity in the proximity of the glass transition (see inset plot).

stability against crystallization in the vicinity of T_g and therefore became a valid tool to study enthalpy changes in aged metallic glasses only after the discovery of BMG compositions, i.e., in the 1990s.^{26,28,29} Today this is considered the most reliable method to study the thermodynamic state of an aging metallic glass system; see, for example, Refs. 10, 16 and 18.

One should emphasize here that the isothermal experimental methods mentioned before to detect viscosity, length and enthalpy relaxation are based on data taken in situ and have a restricted measuring time window from several minutes to a maximum of 2 or 3 days. Like any other isothermal measurement of macroscopic properties, they require an exceptionally good signal-to-noise ratio and an exceptional instrument stability to detect changes on a shorter timescale on one side and the broad tail of the relaxation spectrum at long timescales on the other side. In contrast, the experimental method of the enthalpy recovery allows the observation of enthalpy changes caused by physical aging ex post facto without relying on direct measurements of isothermal signals.

Recently, we have used this method to experimentally detect the time evolution of the enthalpy changes involved during physical aging of an Au-based BMG by applying a wide range of annealing times, from less than 1 s up to several days.¹⁸ The study took advantage of the fast detection response of the fast scanning calorimetry using a chip-calorimeter.³⁰ The results are shown in Fig. 4 for indicated annealing temperatures, which are in the range between 50 and 20K below T_g . The high temperature data are adequately reproduced with a single stretched-exponential decay of the KWW

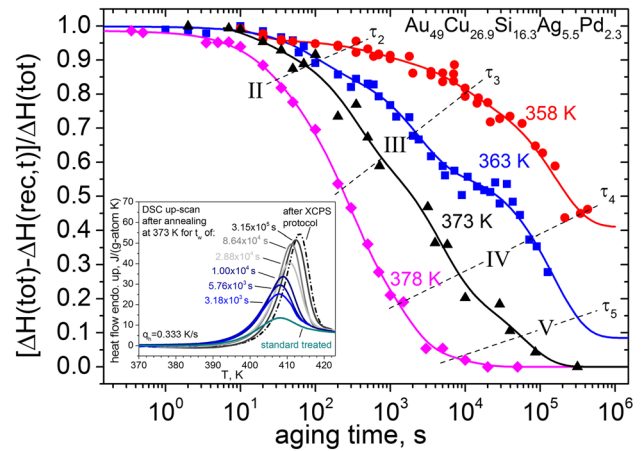


Fig. 4. Time evolution of the enthalpy recovery for the $Au_{49}Cu_{26.9}Si_{16.3}Ag_{5.5}Pd_{2.3}$ BMG, after Ref. 18. The continuous lines are the fits to a sum of exponential decays with average relaxation time τ_i . Inset: Selected enthalpy recovery signals. The excess area with respect to the standard treated sample is a quantitative measure of the recovered enthalpy after aging.

form, whereas at lower temperatures the enthalpy relaxation decay clearly splits into multiple steps, which is modeled in Ref. 18 as a sum of simple exponential decays. This multiple-step enthalpy relaxation pathway results from the separation of the timescales for relaxation at low temperature and thus represents an activation energy spectrum for relaxation. It is also in agreement with some abnormal calorimetric features detected during sub- T_g annealing in other metallic glass systems, e.g., in Refs. 31–35, and with numerous calorimetric studies on other fragile non-metallic glass formers,^{36–38} indicating a universal behavior of the aging glassy state independent of the nature of the atomic bonding.

The hierarchical mechanism of the relaxation pathway is the subject of a long debate. Already in the early 1980s, it was recognized that, although equilibrium thermodynamics cannot be strictly applied to the relaxation of a complex metastable system, the concept of a local equilibrium within a restricted energy range can be used.³⁵ The activation energy spectrum for relaxation is understood to be representative of a complex system of energy wells involving the activated motion of atoms or group of atoms. In the framework of the potential energy landscape approach,³⁹ the observed relaxation process in Fig. 4 is ascribed to transitions from a high-energy local minimum to energetically lower, more deeply relaxed states.¹⁸ We can argue, like in Ref. 35, that in the frozen-in structure there is a tendency of a process involving low activation energy being surrounded by processes with relatively high activation energies, and therefore at a given energy it is favorable to establish a local equilibrium.

MICROSCOPIC FEATURES OF PHYSICAL AGING

The physical aging leads to structural changes at the microscopic level of glassy materials.⁴⁰ Nowadays, large effort is devoted to establishing a clear correlation between the microscopic dynamics and the change of physical properties of the aging metallic glass. The advantage of the metallic glasses is that detailed microscopic information on the collective atomic motion during aging can be obtained by using quite a few techniques such as radiotracer diffusion experiments,⁴¹ positron annihilation lifetime spectroscopy,⁴² nuclear magnetic resonance^{43–45} and the Synchrotron techniques based on the x-ray photon correlation spectroscopy (XPCS)⁴⁶ and high intensity x-ray scattering.⁴⁷

Recent atomistic investigations have revealed that in the metallic glass structure the development of chemical short-range order drives low-temperature equilibration, whereas the relaxation processes responsible for the macroscopic flow are related to irreversible changes in the topological short-to-medium-range order.^{42,48}

The newly developed XPCS technique^{46,49} especially allows us to study the dynamics of metallic liquids in the ultra-viscous state and provides a direct measurement of the microscopic relaxation time necessary for structural rearrangements at the atomic level, which is the aforementioned α -relaxation time τ . With the XPCS technique, it was observed that the structural relaxation processes underlying aging in fragile BMG systems are intermittent and highly heterogeneous^{18,32} and also that long-time annealing can result in trapping the glass configuration in a deep local energy minimum.¹⁸ It was also noticed that even close to T_g , where τ is fast, e.g., 10 s, the atomic dynamics are stationary and persistent for annealing times many orders of magnitude greater than τ .¹⁸ This surprising behavior strongly contradicts previous macroscopic measurements, where aging close to T_g occurs on timescales similar to the structural relaxation time and strengthens the idea of a strong length scale dependence of the dynamics in the glassy state.

A diffusion process on the order of one atomic displacement in metallic glasses can involve thermally activated, highly cooperative atomic motions of 10–20 atoms in a chainlike manner.⁵⁰ In addition, bulk metallic glass-forming systems are typically multicomponent systems characterized by large atomic mismatch among the atomic species.⁵ Thus, it is expected that at low temperature where there are fewer active degrees of freedom, some of the more sluggish relaxation processes, which are controlled by the slower diffusive species, could stay frozen, leading to a more visible separation of the equilibration modes, as is observed in Fig. 4. This is especially true for moderately and highly fragile glass-forming liquids, where the non-Arrhenius behavior, well described by the VFT equation of

the relaxation times, is very steep, and thus there are several orders of magnitude of relaxation time to overcome between the frozen-in structure and the equilibrium liquid.

Figure 5a shows the distinct activation energy spectrum of enthalpy relaxation modes obtained for the $\text{Au}_{49}\text{Cu}_{26.9}\text{Si}_{16.3}\text{Ag}_{5.5}\text{Pd}_{2.3}$ BMG from the enthalpy recovery data of Fig. 4 (filled squares) in comparison with XPCS data (open triangles). The results suggest that the different activation energies are connected to the activation energies for diffusion of the different size atomic species in the alloy. This picture is in agreement with previous radiotracer experiments,^{51–54} as for example those shown in Fig. 5b for the $\text{Zr}_{41.2}\text{Ti}_{13.8}\text{Cu}_{12.5}\text{Ni}_{10.0}\text{Be}_{22.5}$ alloy.⁵⁴ The plot depicts structural α -relaxation time τ data (●, ■, +) that are proportional to the equilibrium viscosity and represent the typical time, τ_D , for displacement or hopping of the largest atom, Zr, over one atomic distance in the alloy. The relation between the equilibrium viscosity and this relaxation time holds over many orders of magnitude for the large atoms.⁵⁴ The other symbols represent the hopping times deduced from radiotracer diffusion experiments from smaller atoms in the alloy according to $\tau_D = l^2/(6D)$, where D is the diffusion coefficient for the species and l the average atomic diameter. The symbols of the smaller atoms represent data for Ni (◇), Co (▽) and Al (□). Data for Be (×) are taken from NMR experiments.⁴⁴ The diffusivity of the large Zr atoms decouples from the diffusivity of the smaller components, and the activation energy for diffusion (slope of data) decreases as the size of the component decreases. This decoupling increases with increasing undercooling to more than four orders of magnitude at T_g (620 K). This tremendous asymmetry in the mobility of the different species during aging must also be present in the Au-based alloy (Figs. 4, and 5a) and therefore be the reason for the broad spectrum of activation energies for the enthalpy as shown in Fig. 5a.

Additionally, we have recently reported that the τ values measured with the $\text{Au}_{49}\text{Cu}_{26.9}\text{Si}_{16.3}\text{Ag}_{5.5}\text{Pd}_{2.3}$ BMG in XPCS during a quasi-static cooling protocol (blue open triangles in Fig. 5a) show a distinct change in the temperature dependence at a well-defined temperature, T_c .⁵⁵ The observed crossover during cooling is the signature of the transition from a kinetically highly fragile to a stronger liquid, and the T_c lies below the conventional calorimetric T_g . This implies that the frozen-in state during processing has retained the structure of the high-temperature fragile liquid and that during annealing the system is driven to equilibrate into a new, stronger liquid.¹⁸ This process involves kinetics with relaxation times of the order of thousands of seconds.^{18,55} The transition is reversible (i.e., strong to fragile) upon re-heating, marked by a small value of the entropy change [~ 0.2 J/(g-atom K)].¹⁸ This value is as low as 2.4% of the entropy of fusion of

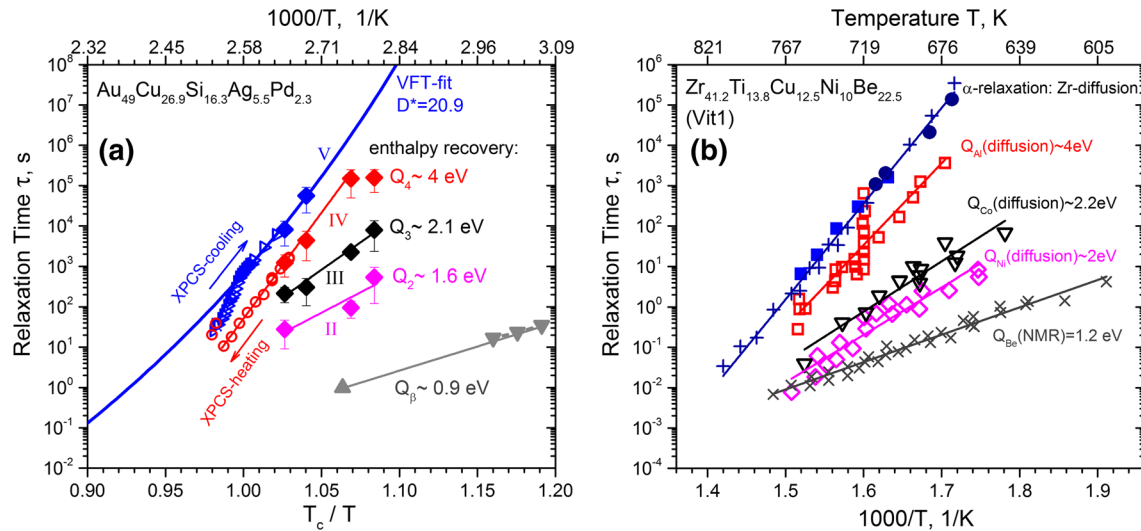


Fig. 5. Temperature dependence of the characteristic relaxation time τ values. (a) Data for the $\text{Au}_{49}\text{Cu}_{26.9}\text{Si}_{16.3}\text{Ag}_{5.5}\text{Pd}_{2.3}$ BMG obtained from the enthalpy recovery spectrum analysis,¹⁸ the β -relaxation study⁴⁷ and the XPCS experiment.^{18,55} T_c is the critical temperature for the liquid-liquid transition. The continuous line is the VFT-fit for the α -relaxation. The straight lines are the Arrhenius fits with the activation energies Q_i . (b) Data for the Zr-based Vit1 for the α -relaxation (filled symbols) in comparison to characteristic diffusion times for different size species in the alloy (open symbols), from Refs. 44 and 54.

this system, and it is the reason why the associated transition temperature is found for $\text{Au}_{49}\text{Cu}_{26.9}\text{Si}_{16.3}\text{Ag}_{5.5}\text{Pd}_{2.3}$ at a very low temperature, which is slightly below the glass transition temperature observed on the typical laboratory timescale.

CONCLUSION

The change of physical properties during aging is mostly observed to be non-exponential in nature, characteristic of stretched dynamic responses. The hierarchical mechanism of the relaxation pathway, proposed almost 50 years ago, is now possible to be verified experimentally because of the new sophisticated and improved tools at hand such as chip calorimetry and increasingly brilliant Synchrotron facilities. Recently, the scenario of a strong length scale dependence of the microscopic dynamics in the glassy state has emerged, which relativizes previous macroscopic measurements where aging close to T_g occurs on timescales similar to the intrinsic relaxation time. Studies based on the XPCS technique show that the structural relaxation processes that underlie aging in metallic glass-forming systems are intermittent and highly heterogeneous. Long-time annealing can result in trapping the glass configuration in a deep local energy minimum and even in leading to structural crossovers from a fragile to a strong liquid.¹⁸

ACKNOWLEDGEMENTS

The authors acknowledge the German Research Foundation (DFG) for support (GA1721/2-2, BU2276/6-2). We are furthermore grateful for collaborations and discussions with Z. Evenson, B. Ruta, D. Cangialosi, M. Stolpe, S. Hechler, O. Gross, L. Schmitt and A. Masuhr.

REFERENCES

1. A.L. Greer, *Nature* 366, 303 (1993).
2. C.A. Angell, *Science* 267, 1924 (1995).
3. C.A. Angell, *MRS Bull.* 33, 544 (2008).
4. I. Gallino, J. Schroers, and R. Busch, *J. Appl. Phys.* 108, 63501 (2010).
5. R. Busch and I. Gallino, *JOM* (2017). doi:10.1007/s11837-017-2574-5.
6. T.A. Waniuk, R. Busch, A. Masuhr, and W.L. Johnson, *Acta Mater.* 46, 5229 (1998).
7. R. Busch, E. Bakke, and W.L. Johnson, *Acta Mater.* 46, 4725 (1998).
8. R. Busch, W. Liu, and W.L. Johnson, *J. Appl. Phys.* 83, 4134 (1998).
9. B. Bochtler, O. Gross, I. Gallino, and R. Busch, *Acta Mater.* 118, 129 (2016).
10. Z. Evenson and R. Busch, *Acta Mater.* 59, 4404 (2011).
11. O. Gross, B. Bochtler, M. Stolpe, S. Hechler, W. Hembree, R. Busch, and I. Gallino, *Acta Mater.* 132, 118 (2017).
12. Z. Evenson, T. Schmitt, M. Nicola, I. Gallino, and R. Busch, *Acta Mater.* 60, 4712 (2012).
13. S.L. Philo, J. Heinrich, I. Gallino, R. Busch, and J.J. Kruzic, *Scr. Mater.* 64, 359 (2011).
14. S. Stanojevic, I. Gallino, H. Aboufadel, M. Sahin, F. Mücklich, and R. Busch, *Acta Mater.* 102, 176 (2016).
15. G.J. Fan, H.-J. Fecht, and E.J. Lavernia, *Appl. Phys. Lett.* 84, 487 (2004).
16. I. Gallino, M.B. Shah, and R. Busch, *Acta Mater.* 55, 1367 (2007).
17. G.J. Fan, J.F. Löffler, R.K. Wunderlich, and H.J. Fecht, *Acta Mater.* 52, 667 (2004).
18. I. Gallino, D. Cangialosi, Z. Evenson, L. Schmitt, S. Hechler, M. Stolpe, and B. Ruta, *ArXiv*. 1706.03830 (2017).
19. R. Böhmer, K.L. Ngai, C.A. Angell, and D.J. Plazek, *J. Chem. Phys.* 99, 4201 (1993).
20. C.A. Angell, K.L. Ngai, G.B. McKenna, P.F. McMillan, and S.W. Martin, *J. Appl. Phys.* 88, 3113 (2000).
21. A. Kovacs, *Fortsch. Hochpolym. Fo.* 3, 394 (1963).
22. A.Q. Tool, *J. Am. Chem. Soc.* 29, 240 (1946).
23. O. Narayanaswamy, *J. Am. Ceram. Soc.* 54, 491 (1971).
24. D. Cangialosi, *J. Phys. Condens. Matter* 26, 153101 (2014).
25. R. Richert, *J. Phys. Condens. Matter* 14, 703 (2002).
26. P. Tuinstra, P.A. Duine, J. Sietsma, and A. van der Beukel, *Acta Metall. Mater.* 43, 2815 (1995).

27. Z. Evenson, I. Gallino, and R. Busch, *J. Appl. Phys.* 107, 1 (2010).
28. R. Busch and W.L. Johnson, *Appl. Phys. Lett.* 72, 2695 (1998).
29. K. Samwer, R. Busch, and W.L. Johnson, *Phys. Rev. Lett.* 82, 580 (1999).
30. C. Schick and V. Mathot, *Fast Scanning Calorim.* (2016).
31. L. Hu, Y. Yue, and C. Zhang, *Appl. Phys. Lett.* 98, 81904 (2011).
32. Z. Evenson, B. Ruta, S. Hechler, M. Stolpe, E. Pineda, I. Gallino, and R. Busch, *Phys. Rev. Lett.* 115, 1 (2015).
33. Y. Fan, T. Iwashita, and T. Egami, *Phys. Rev. Lett.* 115, 1 (2015).
34. H.S. Chen, A. Inoue, and T. Masumoto, *J. Mater. Sci.* 20, 2417 (1985).
35. M.R.J. Gibbs, M.R.J. Gibbs, J.E. Evetts, J.E. Evetts, J.A. Leake, and J.A. Leake, *J. Mater. Sci.* 18, 278 (1983).
36. R.C. Welch, J.R. Smith, M. Potuzak, X. Guo, B.F. Bowden, T.J. Kiczanski, D.C. Allan, E.A. King, A.J. Ellison, and J.C. Mauro, *Phys. Rev. Lett.* 110, 265901 (2013).
37. D. Cangialosi, V.M. Boucher, A. Alegría, and J. Colmenero, *Phys. Rev. Lett.* 111, 095701 (2013).
38. A. Brunacci, J.M.G. Cowie, R. Ferguson, and I.J. McEwen, *Polymer (Guildf)*. 38, 3263 (1997).
39. A. Heuer, *J. Phys. Condens. Matter* 20, 373101 (2008).
40. T. Egami, *Ann. N.Y. Acad. Sci.* 371, 238 (1981).
41. S.W. Basuki, F. Yang, E. Gill, K. Raetzke, A. Meyer, and F. Faupel, *Phys. Rev. B—Condens. Matter Mater. Phys.* 95, 24301 (2017).
42. Z. Evenson, T. Koschine, S. Wei, O. Gross, J. Bednarcik, I. Gallino, J.J. Kruzic, K. Rätzke, F. Faupel, and R. Busch, *Scr. Mater.* 103, 14 (2015).
43. W. Xu, M.T. Sandor, Y. Yu, H.-B. Ke, H.-P. Zhang, M.-Z. Li, W.-H. Wang, L. Liu, and Y. Wu, *Nat. Commun.* 6, 7696 (2015).
44. X. Tang, U. Geyer, R. Busch, W.L. Johnson, and Y. Wu, *Nature* 402, 160 (1999).
45. X.-P. Tang, R. Busch, W.L. Johnson, and Y. Wu, *Phys. Rev. Lett.* 81, 5358 (1998).
46. A. Madsen, A. Flueraşu, and B. Ruta, in *Synchrotron Light Sources Free. Lasers* (Cham: Springer International Publishing, 2015), pp. 1–21.
47. Z. Evenson, S.E. Naleway, S. Wei, O. Gross, J.J. Kruzic, I. Gallino, W. Possart, M. Stommel, and R. Busch, *Phys. Rev. B—Condens. Matter Mater. Phys.* 89, 1 (2014).
48. V.M. Giordano and B. Ruta, *Nat. Commun.* 7, 1 (2016).
49. B. Ruta, Y. Chushkin, G. Monaco, L. Cipelletti, E. Pineda, P. Bruna, V.M. Giordano, and M. Gonzalez-Silveira, *Phys. Rev. Lett.* 109, 1 (2012).
50. F. Faupel, W. Frank, M.P. Macht, H. Mehrer, V. Naundorf, K. Rätzke, H.R. Schober, S.K. Sharma, and H. Teichler, *Rev. Mod. Phys.* 75, 237 (2003).
51. U. Geyer, W.L. Johnson, S. Schneider, Y. Qiu, and T.A. Tombrello, *Appl. Phys. Lett.* 69, 2492 (1996).
52. E. Budke, P. Fielitz, M.P. Macht, V. Naundorf, and G. Froberg, *Defect Diffus. Forum* 143–147, 825 (1997).
53. A. Bartsch, K. Raetze, A. Meyer, and F. Faupel, *Phys. Rev. Lett.* 104, 195901 (2010).
54. A. Masuhr, T. Waniuk, R. Busch, and W. Johnson, *Phys. Rev. Lett.* 82, 2290 (1999).
55. S. Hechler, B. Ruta, M. Stolpe, E. Pineda, Z. Evenson, O. Gross, W. Hembree, A. Bernasconi, R. Busch, and I. Gallino, *ArXiv*. 1704, 06703 (2017).